References and Notes

1. L. W. Alvarez, W. Alvarez, F. Asaro, H. V. Michel, *Science* **208**, 1095 (1980).
2. ———, *Geol. Soc. Am. Spec. Pap. 190* (1982), p. 305.
3. L. T. Silver and P. H. Schultz, Eds., *Geol. Soc. Am. Spec. Pap. 190* (1982).
4. J. Smit and J. Hertogen, *Nature (London)* **285**, 198 (1980).
5. F. T. Kyte, Z. Zhou, J. T. Wasson, *ibid.* **288**, 651 (1980).
6. K. J. Hsü *et al.*, *Science* **216**, 249 (1982).
7. C. B. Officer and C. L. Drake, *ibid.* **219**, 1383 (1983).
8. M. L. Keith, *Geochim. Cosmochim. Acta* **46**, 2621 (1982).
9. D. M. McLean, *Nature (London)* **287**, 760 (1980).
10. M. R. Rampino, *Geol. Soc. Am. Spec. Pap. 190* (1982), p. 455.
11. C. P. Strong, *N.Z. J. Geol. Geophys.* **20**, 687 (1977).
12. H. Palme, *Geol. Soc. Am. Spec. Pap. 190* (1982), p. 223.
13. J. S. Gilmore, J. D. Knight, C. J. Orth, C. L. Pillmore, R. H. Tschudy, *Nature (London)* **307**, 224 (1984).

14. We thank D. S. Russell and F. Asaro for providing background iridium data for nonboundary material from the Woodside Creek stratigraphic column.

3 May 1984; accepted 17 July 1984

Ultrahigh Pressure: Beyond 2 Megabars and the Ruby Fluorescence Scale

Abstract. *A new design of the diamond-window, high-pressure cell has permitted static pressure of 2.8 megabars to be generated for the first time. The design is unusually stable mechanically, and thus it should be possible to use the new cell to study most materials, including hydrogen, in the unexplored pressure region above 1 megabar.*

The generation of static high pressures of several megabars for laboratory experimentation has been an important goal for materials science. At pressures exceeding 1 Mbar, the energy equivalent is on the order of the minimum required to convert many materials from insulator or semiconductor states to the metallic state. Ross and McMahan predicted (*1*) that hydrogen, for example, would become a high-temperature (greater than 25°C) superconductor at megabar pressures. In the present study new designs of high-pressure apparatus have been used successfully in maintaining ruby-plus-metal composite samples stably at 2.8 Mbar without apparatus failure. This result constitutes a major advance over the earlier maximum, which was limited to 1.7 Mbar (*2*).

The quest to reach megabar pressures in order to observe metallic and other behavior of materials has benefited from the use of apparatus in which single-crystal diamonds are integral, strong component parts. Diamonds have served as windows for radiation transmitted and emitted in interactions with samples held under pressure (*2*). The ability to study a pressurized sample in situ by spectroscopic methods has been crucial in modern high-pressure research.

The ultimate strength of diamonds at very high pressures has become a major design consideration. Analysis of the diamonds that flowed and those that did not flow under the same experimental conditions in other experiments suggested that impurity levels of nitrogen inclusions could be important (*2*). Some diamonds contain ~700 parts per million of nitrogen. Diamonds in which nitrogen platelets were present, as determined by high-sensitivity Fourier-transform infrared analysis (*3*), were selected for the

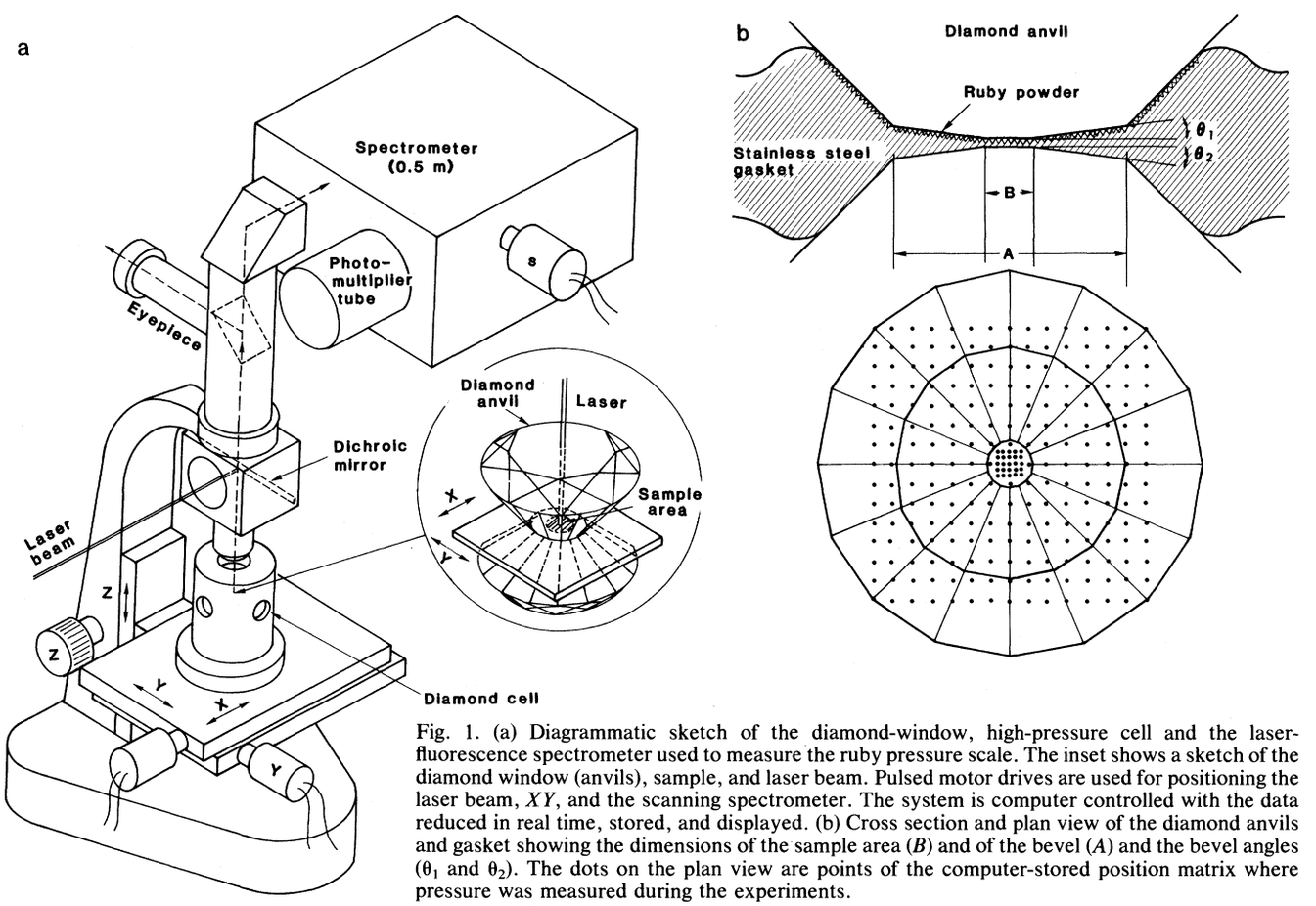

Fig. 1. (a) Diagrammatic sketch of the diamond-window, high-pressure cell and the laser-fluorescence spectrometer used to measure the ruby pressure scale. The inset shows a sketch of the diamond window (anvils), sample, and laser beam. Pulsed motor drives are used for positioning the laser beam, *XY*, and the scanning spectrometer. The system is computer controlled with the data reduced in real time, stored, and displayed. (b) Cross section and plan view of the diamond anvils and gasket showing the dimensions of the sample area (*B*) and of the bevel (*A*) and the bevel angles (θ_1 and θ_2). The dots on the plan view are points of the computer-stored position matrix where pressure was measured during the experiments.

present study. Our results tend to confirm that diamonds with nitrogen platelets are stronger than those without.

Successful experiments to generate static pressures above 1 Mbar have resulted from the analysis of stress distributions on diamond surfaces in contact with the gasket region and sample chamber in high-pressure apparatus. Bevels that are ground on diamond anvils are designed to avoid sharp stress gradients at high pressure. We tested new experimental bevel angles, sample areas, and diamond alignments to determine conditions that would be most favorable in the cell at the highest pressures.

The experimental design of the high-pressure cell is similar to that of the one described by Mao *et al.* (*2*). Two sets of modified, brilliant-cut gemstone diamonds were used in the experiments. The design parameters were as follows (Fig. 1, a and b, shows a representation): A = 300 μm, B = 50 μm; the bevel angles in anvil set 1 were $\theta_1 = 0°$ and $\theta_2 = 7°$; the angles in anvil set 2 were $\theta_1 = 5°$ and $\theta_2 = 5°$. The included angles, $\theta_1 + \theta_2$, were larger than those used in past experiments (5°) as was the A/B ratio. Bruno and Dunn (*4*) calculated that large bevel angles would lead to a more stable stress distribution in diamond anvils. Our results confirm that general conclusion.

We formed the sample by pressing powdered ruby crystals into a full work-hardened T301 stainless steel plate that had an initial thickness of 0.25 mm. The plate was preindented at a central pressure of 300 kbar. The indented plate then served as the sample and, as it extruded, as the supporting gasket as well. An automated system described by Mao *et al.* (*6*) was used to focus a helium-cadmium laser beam at points of a preselected grid (Fig. 1b). The laser beam sampled a cross section with a diameter of 5 μm. Points were separated by 25 μm in the large grid and by 7 μm across the flat diamond surface. At each point of the grid the laser beam focused on a ruby crystal or group of crystals. Laser-induced fluorescence of the ruby crystals was observed spectrally as a sequence of the automated system. Pressure was measured at a total of 40,000 points during the series of experiments. Pressure was determined with reference to the calibrated shift of the ruby R_1 emission line (*6*). As a backup calibration, the loading force (*2*) was measured as well. The area could be measured and the pressure distribution determined to calculate the pressure.

Measurements were made with anvil sets 1 and 2. The first experiments with anvil set 1, which had slightly larger bevel angles and A/B ratio than the earlier 1.7-Mbar design (*2*), reached a maximum pressure of 1.85 Mbar. The experiment terminated as one diamond anvil exploded. The cause of the failure was that the gradient was steep at the outer edge of the bevel, falling from 800 kbar to less than 50 kbar in 25 μm. The bevel angle was adjusted in anvil set 2 to lower the edge pressure. The diamond anvils showed no evidence of plastic deformation as the pressure was raised to 1.85 Mbar.

The radial pressure distribution in the cell was considerably more favorable in the experiments with diamond-anvil set 2 than those with set 1. The maximum pressure on the sample exceeded 2.8 Mbar and could have been raised further. Pressure was measured in the flat surface and bevel regions of the diamond-window cell in this set, as with anvil set 1. Anvil set 2 benefited from the higher included bevel angle (10° in anvil set 2 versus 7° in anvil set 1). The experiments were successful and were not terminated as a result of the failure of the diamonds. No flow was apparent as observed under the microscope during and after the experiment, even though the apparatus was held stably at pressures over 2 Mbar for 40 days while data were being collected.

An unusual phenomenon occurred as the maximum pressure was raised above 1.8 Mbar with both sets of diamond anvils. Emission of the R lines of the ruby crystals gradually diminished in intensity. In the experiments with anvil set 2 at pressures above 1.8 to 1.9 Mbar, the R line emission could not be detected at all; this result suggests that the emission yield threshold for the chromium ion in ruby had become unfavorable. At about 1.2 Mbar, a very strong emission appeared in ruby crystals at shorter wavelengths. This emission was observed as a shoulder that swept through the visible spectral region as pressure was increased. Between 1.2 and 1.8 Mbar, the emission tail superimposed the ruby R lines as they were diminishing. Above 1.8 Mbar in the experiment with anvil set 2, pressure was determined independently in the absence of the ruby R lines.

Two methods were used to determine the maximum pressure. In the first method we used the loading force to trace the average pressure of the central area (5 μm in diameter) of the cell defined by the laser beam in the experiments with anvil set 2 (Fig. 2a); the pressure at several radial distances from the center is also plotted versus the mechanical force applied to the diamond anvils. Pressures up to 1.8 Mbar in the central area were measured by the ruby fluorescence scale. At pressures above 1.8

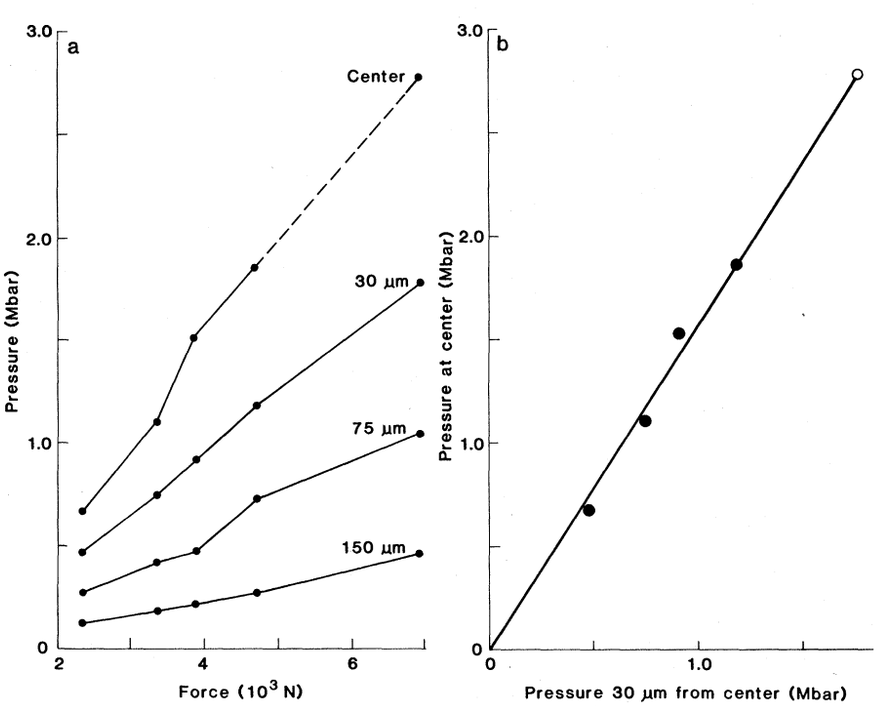

Fig. 2. (a) Plot of pressure versus applied force in the diamond-window, high-pressure cell as a function of distance from the center of the sample area. (b) Plot of pressure at the center of the sample area of the high-pressure cell versus pressure at a radial distance of 30 μm from the center.

Mbar a linear extrapolation (dashed line) to a maximum loading force of 7000 N produced a central pressure of 2.8 Mbar. This method is similar but superior to conventional methods of ultrahigh-pressure calibration because it incorporates supporting data at radial distances.

In the second method the maximum pressure was determined from the pressure distribution by calculation of the ratio of the pressure at a radial distance of 30 μm to the pressure at the center of the flat region. An important factor associated with using the ratio in these calculations is that the flat diamond surface did not undergo plastic deformation. This ratio was constant for anvil set 2 at several central pressures up to 1.8 Mbar (Fig. 2b). The resulting maximum pressure in the central area of anvil set 2 was thus determined independently of the loading force to be 2.8 Mbar when pressure at the 30-μm radius was 1.8 Mbar.

The design of anvil set 2 was found to have exceptional properties. Pressure could be raised smoothly to above 2 Mbar after alignment procedures. The conditions were unusually stable; the pressure in the sample region did not vary perceptibly during the 40-day period of the experiment. Unloading the pressure slowly did not produce as favorable stress distributions as loading the pressure, but the diamond anvils were reclaimed after the experiment. These results with a composite of stainless steel and ruby crystals suggest that it should be possible to pressurize any other gasketed materials stably for study at 2 to 3 Mbar with this apparatus, including solids normally in the gaseous state at 1 bar such as hydrogen.

P. M. Bell
H. K. Mao
K. Goettel

Geophysical Laboratory,
Carnegie Institution of Washington,
Washington, D.C. 20008

References

1. M. Ross and A. K. McMahan, in *Physics of Solids Under Pressure*, J. S. Schilling and R. N. Shelton, Eds. (North-Holland, New York, 1981), pp. 161–174.
2. H. K. Mao, P. M. Bell, K. J. Dunn, R. M. Chrenko, R. C. DeVries, *Rev. Sci. Instrum.* **50**, 1002 (1979); H. K. Mao and P. M. Bell, *Science* **203**, 1004 (1979).
3. H. K. Mao, P. M. Bell, J. Xu, P. T. T. Wong, *Carnegie Inst. Washington Yearb.* **82**, 419 (1983).
4. M. S. Bruno and K. J. Dunn, in *High Pressure in Science and Technology* (Elsevier, New York, in press).
5. H. K. Mao, C. Hadidiacos, P. M. Bell, K. A. Goettel, *Carnegie Inst. Washington Yearb.* **82**, 421 (1983).
6. H. K. Mao, P. M. Bell, J. Shaner, D. Steinberg, *J. Appl. Phys.* **49**, 3276 (1978).

24 July 1984; accepted 14 September 1984

Cyclophilin: A Specific Cytosolic Binding Protein for Cyclosporin A

Abstract. *Cyclophilin, a specific cytosolic binding protein responsible for the concentration of the immunosuppressant cyclosporin A by lymphoid cells, was purified to homogeneity from bovine thymocytes. Cation-exchange high-performance liquid chromatography resolved a major and minor cyclophilin species that bind cyclosporin A with a dissociation constant of about 2 × 10^{-7} moles per liter and specific activities of 77 and 67 micrograms per milligram of protein, respectively. Both cyclophilin species have an apparent molecular weight of 15,000, an isoelectric point of 9.6, and nearly identical amino acid compositions. A portion of the NH_2-terminal amino acid sequence of the major species was determined. The cyclosporin A–binding activity of cyclophilin is sulfhydryl dependent, unstable at 56°C and at pH 4 or 9.5, and sensitive to trypsin but not to chymotrypsin digestion. Cyclophilin specifically binds a series of cyclosporin analogs in proportion to their activity in a mixed lymphocyte reaction. Isolation of cyclophilin from the cytosol of thymocytes suggests that the immunosuppressive activity of cyclosporin A is mediated by an intracellular mechanism, not by a membrane-associated mechanism.*

Cyclosporin A, a cyclic undecapeptide of fungal origin is a potent immunosuppressant with low myelotoxicity (*1*). It is used to prevent rejection of kidney and liver transplants (*2*) and in graft versus host disease (*3*). Additional studies suggest applications for cyclosporin A in treatment of autoimmune diseases (*4*), and schistosomiasis (*5*). Cyclosporin A also provides a unique probe of the biochemical factors involved in regulation of the immune and possibly other physiological responses.

Cyclosporin A appears to act on the immune system by inhibiting the initial steps of T-lymphocyte activation. It diminishes the responsiveness of helper-inducer T lymphocytes to interleukin-1 (IL-1) (*6*, *7*). Cyclosporin A also inhibits the production of interleukin-2 (IL-2) by alloantigen- and lectin-stimulated T lymphocytes (*7–10*) and prevents the expression of receptors for IL-2 by precursor cytolytic T lymphocytes (*9*, *11*). However, cyclosporin A has minimal effects on the activation and proliferation of suppressor T lymphocytes (*12*) or on the response of primed T lymphocytes to exogenous IL-2 (*10*, *13*). In addition, cyclosporin A is reported to inhibit γ-interferon production by lymphocytes (*14*) and to suppress delayed-type hypersensitivity reactions and inhibit production of lymphokines that affect macrophage behavior (*15*). However, the specific biochemical mechanism by which cyclosporin A inhibits T-lymphocyte activation and lymphokine production has not been established.

We reported earlier (*16*) that uptake

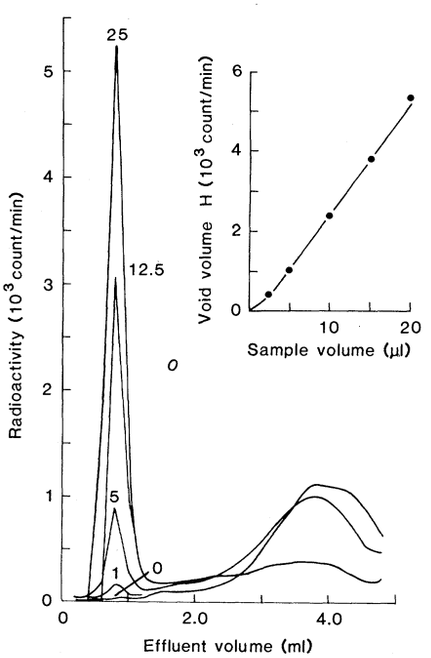

Fig. 1. Sephadex LH-20 column assay for cyclophilin activity. Minicolumns (1.8 ml) of Sephadex LH-20 resin (Pharmacia) were preequilibrated in tris buffer (20 m*M*, *p*H 7.2) containing 2-mercaptoethanol (5 m*M*) and sodium azide (0.02 percent). Samples for assay were diluted to 90 μl with tris buffer containing 7.5 percent newborn calf serum (Gibco) in small glass test tubes. After the addition of 10 μl of [^{3}H]cyclosporin A (50 μg/ml; 0.05 μCi/ml) in 40 percent ethanol, tubes were agitated gently; 50 μl of the sample was applied to the column, and 20 μl was assayed for radioactivity in 5 ml of Liquiscint (New England Nuclear). Columns were eluted with tris buffer, and the fractions were assayed for radioactivity. Data reflect [^{3}H]cyclosporin A elution resulting from complex formation with 0, 2.5, 5.0, 12.5, and 25 μl of a solution of purified cyclophilin (0.7 mg of protein per milliliter). The inset shows that elution of [^{3}H]cyclosporin A through LH-20 columns is proportional to the amount of cyclophilin in the assay. Only the 0.5- to 1.0-ml elutate was assayed for radioactivity in routine assays.